A Study on Double-sided Optical Focusing Alignment of Transparent Substrate

Chia-Lien Ma[a], Chih-Chung Yang, Yu-Hsuan Lin and Kuo-Cheng Huang
Taiwan Instrument Research Institute, National Applied Research Laboratories, 20 R&D RD. VI, Hsinchu, Taiwan
marklin@itrc.narl.org.tw

Keywords: Auto Focus, Optical Inspection, Assembly Error Detection.

Abstract: The non-contact optical focus positioning technology proposed in this study uses the principle of optical imaging to develop a system that is simple, fast, and has a microscopic image inspection function. This study uses a dual optical path design for the upper and lower systems. The near-semi-reflective substrates in the system have different reflectivity coatings. The energy density of the transmitted and reflected light is captured through image processing. The position shift or tilt of the components is then used to calculate the energy density difference of the upper and lower systems. It can be quickly converted into focus position, system uniformity, surface height, component assembly offset and tilt. The technology of this research can overcome the problems of manual focus, additional device focus module and human eye misjudgement, and provide a measurement method and tool with simple operation and high accuracy. It can effectively adjust the Z-axis offset range of the lower system can be effectively adjusted by ±1 mm, the lower system tilts range ±1°, and the substrate tilts range ±1 by the difference of the upper and lower energy densities. The Y-axis offset range is ±0.1 mm by the maximum energy density of the upper system.

1 INTRODUCTION

As semiconductor technology continues to evolve, line widths continue to decrease and manufacturing processes become more complex. At present, the industry has entered the 7 nm process stage and requires nearly a thousand processes. Advanced processes and complex processes are becoming more and more demanding for measuring speed and accuracy, and the demand for automated optical measuring equipment for precision components is increasing.

Automated optical inspection (AOI) is a high-speed and high-precision optical image detection system. It uses machine vision as a detection standard technology to improve the shortcomings of human-based detection (Wang et al, 2019). The application level includes high-tech industry research and development, manufacturing quality control, national defense, life, medical, environmental protection, electricity, etc. AOI is a common detection technique in industrial processes. Optical instruments are used to obtain the surface state of the sample, and image processing technology is used to detect flaws. Because it is non-contact testing, semi-finished products can be inspected during the process (Chon et al, 2001). High-precision optical image detection system, including measurement lens technology, optical lighting technology, focus positioning measurement technology, electronic circuit testing technology, image processing technology and automation technology application, etc., its development and application not only meet the development needs of high-tech industry, but also can be extended to the defence military industry (Zureik et al, 2010). The analysis and research of military weapons manufacturing, night vision combat systems, and strategic topography are closely related to this imaging technology.

Among them, the focus positioning measurement technology is often applied to accurately adjust the image position, and there are many setups and technologies that can apply this technology. The focus positioning measurement system is roughly divided into two kinds of systems. Most of the systems need to be set up with another microscope. When the system focus is confocal with the focal plane of the microscope, the surface image is obtained, and the distance is calculated by geometric

[a] https://orcid.org/0000-0003-4681-0351

principle (Browne et al, 1992)(Maly et al, 1994). However, if the sample is a penetrating material, the reflection signal of the lower interface will be so weak that it is difficult to judge the location of the interface. Therefore, only surface focusing can be performed, and the focused optical path and the microscope imaging optical path are not coaxially designed, so the two focal points cannot overlap. In another system, a chromatic confocal detection module or a laser rangefinder is combined with an external module to perform positioning and single point position measurement. First move the external module to the detection position, define the detection line, and finally detect it (Tiziani et al, 1994)(Kim et al, 2013). In addition, the distance between the two modules needs to be corrected in advance, which requires an additional calibration time, resulting in a slow measurement speed.

In view of the fact that these measurement systems require a human eye, manual focus or an external focus module to obtain a clear position image, it will result in reduced measurement efficiency and accuracy. Therefore, this research develops a measurement module with microscopic image inspection and autofocus function, and has the characteristics of fast, easy operation and high longitudinal measurement range. In this study, a self-developed focusing module was designed, which is designed for dual light paths in the upper and lower systems. Combined with a microscope objective, it features microscopic image detection for quick alignment of measurement locations. Using the principle of optical imaging, the anti-reflective coating of the near-half-reflective substrate allows the energy density of penetration and reflection to be approximately the same at the focal position. By calculating the difference in energy density between the upper and lower systems, which is caused by the shift or tilt of the lower system and the near-half-reflective substrate, the focus position information, system uniformity and surface height can be instantaneously obtained, and fast autofocus operation can be performed. At the same time, after rapid focusing, the assembly error of the system or component can be known by the change in energy density of the upper and lower systems.

2 EXPERIMENTAL PRINCIPLE AND SETUP

A lens is a combination of multiple lenses that correct aberrations such as astigmatism, coma, field curvature, distortion, and spherical aberration by the shape, thickness, and curvature of the lens and the spacing between the lenses. The lens can be viewed as a combination of two spherical surfaces, so the imaging results can be obtained using a single spherical imaging formula. The lens imaging path is shown in Figure 1. It is assumed that the lens is placed in a uniform medium, and the medium is assumed to be air. The light source is irradiated onto the object and refracted through the lens to focus the image.

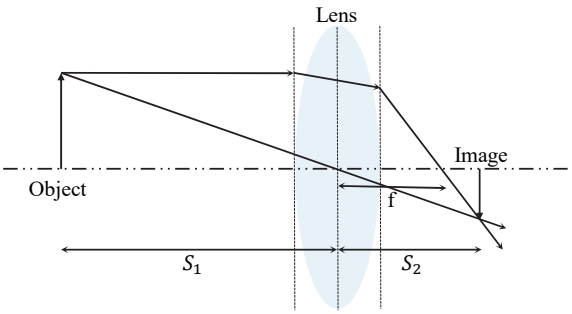

Figure 1: Focus image.

The imaging formula, also known as the lens-maker's formula, is as follows (Nayar and Nakagawa, 1994):

$$\frac{1}{S_1}+\frac{1}{S_2}=\frac{1}{f} \tag{1}$$

where S_1 is the object distance, which is the distance between the object and the lens; S_2 is the image distance, which is the distance between the image and the lens; and f is the focal length of the lens. It can be seen from the lens-maker's that a relative image distance can be obtained from one object distance, and vice versa. When the sample is in the object plane, the outline of the sample is focused by the lens and forms a sharp image. The image at this time is called a focus image. When the sample is not in the object plane, a circle is formed in the image plane according to the trigonometric principle. The blurred image was out of focus at the time.

The optical design is shown in Figure 2. The design concept is the upper and lower double light path. The upper system includes a CCD for capturing images, a focusing microscope objective, and a near-half reflecting substrate. The lower system consists of a light source, a mirror, a CCD and a focusing microscope objective. This model is created by using a single lens to represent the focusing microscope objective lens, and it is selected as a standard product. The purpose is to establish the model in the simplest way. If a good focusing effect can be achieved with this structure, a more accurate result can be obtained

by replacing the focusing microscope objective during actual measurement. Since only surface reflection is considered, the focus position is designed on the lower surface of the near-half reflecting substrate.

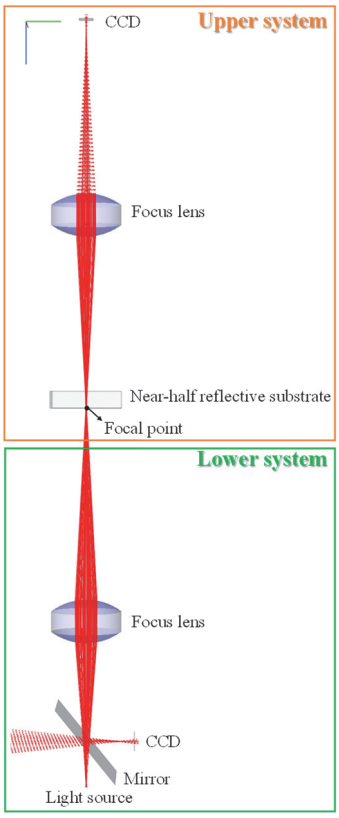

Figure 2: Schematic diagram.

The Figure 2 shows, the light source transmits through the half mirror to the focus lens, focusing on the lower surface of the near semi-reflective substrate, which is the focus position. Due to the dual optical path design, the light will have two paths. A part of the light is reflected by the lower surface and returned to the CCD of the lower system. The other part of the light continues to propagate through the near-half reflecting substrate. After passing through the focusing lens, focus on the CCD of the upper system.

The wavelength of the simulated light source is 550 nm representing the visible light band. The mirror is 50% transmitted and 50% reflective. The lens has a curvature of 10 mm, the thickness is 5 mm, the material is BK7, and no surface coating. The near-half reflecting substrate has a length of 10 mm and a width of 10 Mm, thickness 2 mm, material BK7. In this paper, non-sequential optical tracking does not consider optical wave effects. Because the diffraction and near-field effects caused by the objects in the experimental structure are negligible. In the process of optical simulation, the material and interface have been correctly set, so the calculation of Fresnel equations will be considered and calculated by the FRED optical simulation software.

3 EXPERIMENTAL RESULTS AND DISCUSSION

In order to obtain a clear image when the CCD of the upper and lower systems is in the focus position, the upper surface and the lower surface of the near-half-reflective substrate are coated, which is determined by simulation. The clarity of the image is positively correlated with the optical energy density, so the energy density can be used as a basis for judging the clarity of the image.

The simulation results are shown in Figure 3. First, the reflection and transmittance of pure glass materials are analysed. At the focus position, the energy density received by the upper system is much larger than that received by the lower system, which is about 33.5 times. In other words, in the case where the upper and lower surfaces of the near-half-reflective substrate are not coated, only the upper system can capture a clear image, and the lower system can only receive a very weak and blurred image. In order to improve the excessive difference in energy density between the upper and lower systems, the reflective coatings on the lower surface of the near-half-reflective substrate were simulated at 30%, 60%, and 80%, respectively. Among them, in the case of 30% and 80% reflective coating on the lower surface coating, the difference in energy density between the upper and lower systems is 3.46 and 0.37 times, respectively. Only one of the systems can receive clear images at the focus position, not both systems simultaneously. For both systems to capture a clear image, the lower surface needs to be plated with a 60% reflective coating to receive a clear image at the same time, as shown in Figure 3. This coating specification is ideally feasible, but in fact, the coating quality and mechanism error must also be considered, so it needs to be measured to determine.

In order to calibrate the assembly error of the system and components, the CCD and lens of the above system are used as the reference to simulate the four assembly conditions, which are the lower system is displaced in the Z-axis direction, shifted in the Y-axis direction, the angle θ is tilted with the light source as a centre, and the near-half-reflective substrate is tilted at an angle ψ from the centre of the substrate, as shown in Figure 4.

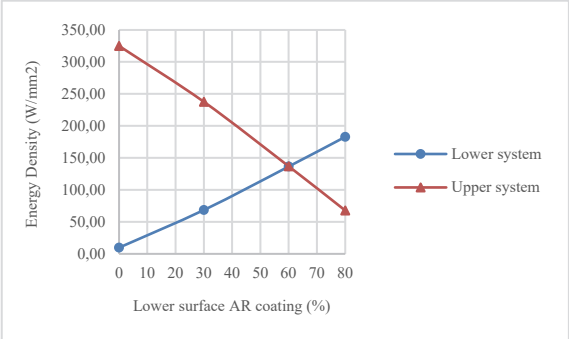

Figure 3: Energy density change plots for different coating systems.

In the case of different reflective coatings, the lower system is offset in the Z-axis direction, and the Z-direction offset can be adjusted by the difference in energy density between the upper and lower systems, and the range is ±1 mm, as shown in Fig. 5 (a). (b), (c) and (d). However, in the case of uncoated, it is difficult to adjust compared to other cases where there is a coating. Wherein, as observed in Figure 5, the left and right curves are asymmetrical because the focus position will be in the near semi-reflective substrate when the lower system is closer to the upper system; when the lower system is far away from the upper system, the focus position will be in the air, and due to the refractive index of the substrate and air are not the same, so the energy density near and away from the system is asymmetric.

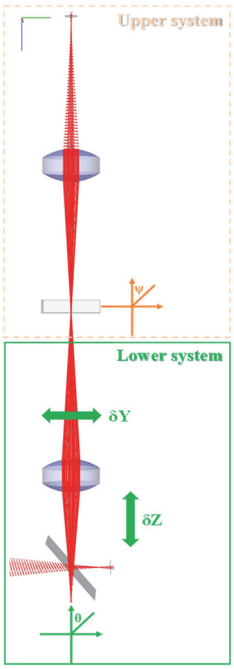

Figure 4: System and component assembly error types.

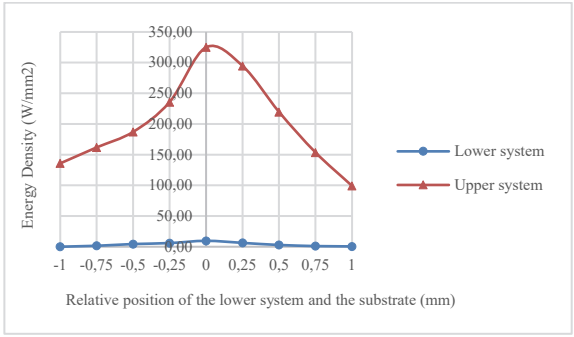

(a)

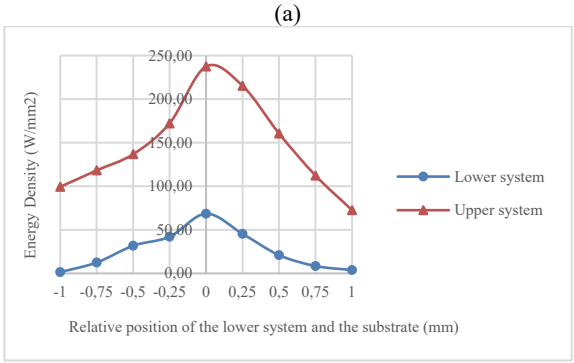

(b)

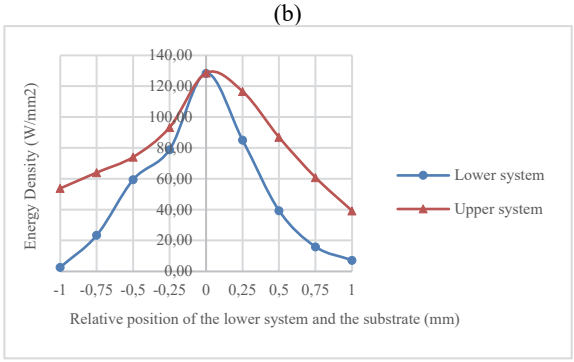

(c)

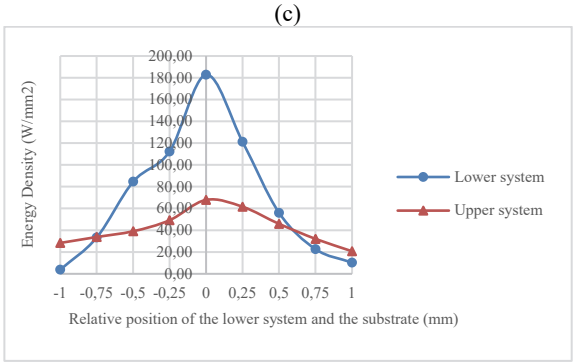

(d)

Figure 5: Substrate (a) uncoated, (b) 30%, (c) 60%, and (d) 80% reflective coating, lower system energy density variation.

Since the energy density of the upper and lower systems can be made the same when the lower surface of the substrate is 60% reflective coating, it is used as

a standard sheet. When the system is offset in the Y direction, the Y-direction offset of the lower system can be adjusted by the maximum energy density of the upper system, and the range is ±0.1 mm, as shown in Figure 6.

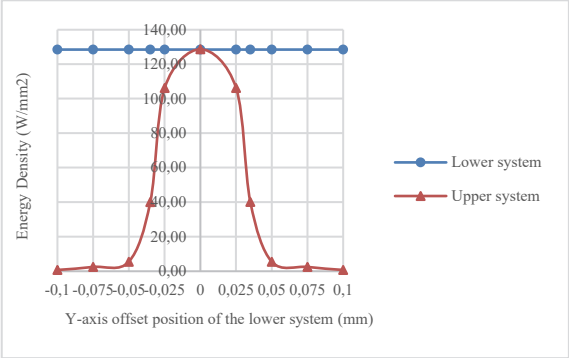

Figure 6: System energy density change diagram under the Y-axis offset of the lower system.

When the lower system tilts the θ angle with the light source as the centre, the tilt of the lower system can be adjusted by the difference in energy density between the upper and lower systems, and the range is ±1˚, as shown in Figure 7.

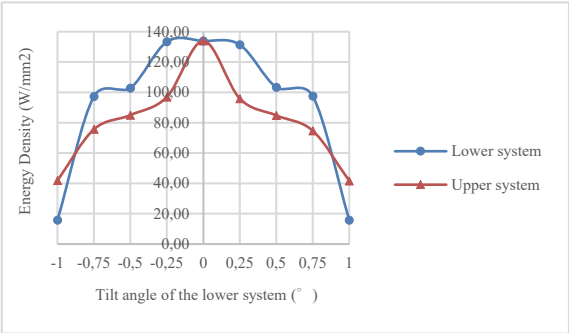

Figure 7: System energy density change diagram at lower system tilt.

When the near-half-reflective substrate is tilted at an angle ψ from the centre of the substrate, the tilt angle can be determined by the change of the energy density of the lower system, and the range is ±1˚, and the substrate uniformity can be detected, as shown in Figure 8.

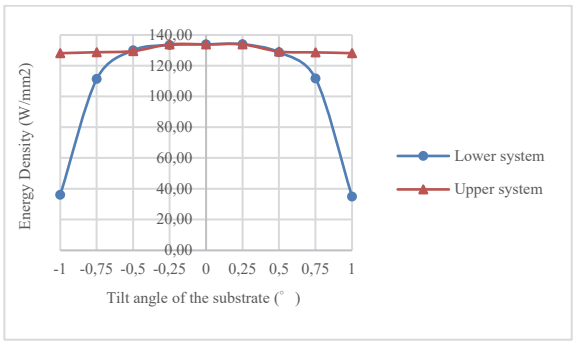

Figure 8: System energy density change diagram of substrate tilt.

Based on the above simulation results, in an actual setup, a power meter and profiler is used to measure the energy density difference between the upper and lower systems. If the energy density of the lower system is greater than the upper system, the tilt angle of the substrate must be adjusted. If the energy density difference is greater than 90, the Y-axis displacement of the lower system must be adjusted; if the energy density difference is greater than 20, the Z-axis displacement of the lower system must be adjusted first; if the energy density difference is less than 20, the tilt of the lower system must be adjusted angle.

4 CONCLUSIONS

The substrate coating simulation results show that the 60% coated substrate is used as the calibration standard film, so that the upper and lower systems can capture clear images. In the assembly error simulation results, the Z-axis offset range of the lower system can be effectively adjusted by ±1 mm, the lower system tilts range ±1˚, and the substrate tilts range ±1 by the difference of the upper and lower energy densities. The Y-axis offset range is ±0.1 mm by the maximum energy density of the upper system. Further, the uniformity of the substrate can be detected as a result of the tilt of the substrate.

The focus positioning technology proposed in this study is a self-developed non-contact optical measurement module that overcomes the problems of the traditional autofocus measurement module and can be widely used in autofocus. It is suitable for single point height, uniform measurement and system assembly error detection of microstructure.

ACKNOWLEDGEMENTS

The authors would like to express their appreciation for financial aid from the Ministry of Science and Technology, R.O.C under grant numbers MOST 108-2221-E-492-019, MOST 108-2218-E-492-010 and MOST 108-2622-E-492-009-CC3. The authors would also like to express their gratitude to the Taiwan Instrument Research Institute of National Applied Research Laboratories for the support.

REFERENCES

Wang, X., Zheng, Z., Fan, Y., Lai, M., Wei, J., Wu, X., "A focus automatic positioning system of high-power laser beam based on plasma ultraviolet radiation," *High Power Laser and Partical Beams*, Vol. 31, 2019.

Chon, S. M., Choi, S. B., Kim, Y. W., Kim, K. W., Lim, K. H., Choi, S. Y., and Jun, C. S., 2001. "Development of automated contact inspection system using in-line CD SEM," IEEE, 399-401.

Zureik, E., Lyon, D., Abu-Laban, Y., *Surveillance and Control in Israel/Palestine: Population, Territory and Power*, Routledge, 2010.

Browne, M. A., Akinyemi, O., and Boyde, A., 1992. "Confocal surface profiling using chromatic aberration," *Scanning*, Vol. 14, 145-153.

Maly, M. and Boyde, A., 1994. "Real-time stereoscopic confocal reflection microscopy using objective lens with linear longitudinal chromatic dispersion," *Scanning*, Vol. 16, 187-192.

Tiziani, H. J., and Uhde, H. M., 1994. "3-Dimensional image sensing by chromatic confocal microscopy," *Appl. Opt.*, Vol. 33, 1838–1843.

Kim, T., Kim, S. H., Do, D., Yoo, H., and Gweon, D., 2013. "Chromatic confocal microscopy with a novel wavelength detection method using transmittance," *OPTICS EXPRESS*, Vol. 21, 6286-6294.

Nayar, S.K., and Nakagawa, Y., "Shape from focus system," 1994. *IEEE*, Vol. 16, 824-831.